XLVI CILAMCE
VITÓRIA - ES - BRAZIL - 2025
XLVI IBERO-LATIN AMERICAN CONGRESS ON COMPUTATIONAL METHODS IN ENGENEERING

Computational Modeling of Aircraft Wing Vibrations Under Turbulent Flow Using an Optimized Tuned Mass Damper (TMD)

João V. O. de Oliveira[1], Marcelo A. da Silva[1],

[1]*Center for Engineering, Modeling, and Applied Social Sciences, Federal University of ABC (UFABC)*
Avenida dos Estados, 5001, 09280-560, Santo André, Brazil
joao.ota@aluno.ufabc.edu.br, joaovictor.ota@gmail.com
[2]*Center for Engineering, Modeling, and Applied Social Sciences, Federal University of ABC (UFABC)*
Avenida dos Estados, 5001, 09280-560, Santo André, Brazil
marcelo.araujo@ufabc.edu.br

Abstract.

In engineering projects, the study and analysis of vibrations is of paramount importance. To minimize the detrimental effects caused by this phenomenon, it is common practice to employ dampers to reduce the impact of resonance and fatigue on structural components. In aircraft wings, such effects are particularly prevalent due to the continuous aerodynamic loads acting on the structure.

This study employs an optimized Tuned Mass Damper (TMD) to mitigate these dynamic loads. A TMD is a device attached to the structure that, through its mass, stiffness, and damping characteristics, dissipates part of the energy transferred to the wing–TMD system.

The Newmark method is used to obtain the numerical solution of the differential equation governing the system's behavior. An optimization algorithm developed in MATLAB is then applied to determine the optimal TMD configuration. Finally, based on the results obtained from the simulations, the feasibility of implementing the TMD in an aircraft wing is assessed.

Keywords: Tuned Mass Damper (TMD); Mechanical Vibrations; Structural Dynamics

1 Introduction

Vibrations are intrinsic to physical systems and have long been a subject of scientific inquiry due to their impact on structural integrity, comfort, and performance. With the advancement of computational modeling and analytical methods, it has become possible to predict, simulate, and control vibrational behavior in complex systems. In modern engineering, vibration analysis is essential for the design of buildings, bridges, power plants, aircraft, and aerospace vehicles. Proper modeling enables engineers to reduce development costs, improve structural safety, and improve user comfort.

In the design of aircraft wings, vibration analysis plays a critical role. Throughout all phases of flight, wings are subjected to various excitations, including inertial loads from maneuvers and atmospheric turbulence. These fluid–structure interactions can lead to dynamic instabilities such as buffeting and flutter. Additionally, resonance and fatigue must be carefully evaluated. Resonance occurs when the excitation frequency aligns with the structure's natural frequency, resulting in amplified displacements that may lead to structural failure. Fatigue arises from cyclic loading, which promotes the initiation and propagation of microcracks that can compromise material integrity over time.

To mitigate these effects, damping systems are commonly employed. Among them, the Tuned Mass Damper (TMD) has proven to be an effective and widely adopted solution in civil, mechanical, and aerospace engineering. The TMD consists of a secondary mass connected to the primary structure through a spring and a damper. When properly tuned, it dissipates a portion of the vibrational energy, thereby reducing the system's response to dynamic loads.

In this study, a simplified aircraft wing model is developed, and an optimized TMD is integrated into the structure. A computational simulation is implemented, where turbulent excitations are represented as discrete gusts applied to the wing. The system's response is evaluated with and without the TMD using a routine developed in MATLAB. The objective is to assess the effectiveness of the optimized TMD in reducing the vibrational energy

of the wing structure.

2 Methods

2.1 Study geometry

The Cessna 172, a widely used single-engine aircraft produced by Cessna Aircraft Company (a Textron Aviation subsidiary), is popular in general aviation for pilot training, recreational flights, business travel, and aerial patrol. Its reliability and safety have made it a benchmark aircraft since its introduction in 1955.

The wing airfoil of this aircraft has been the subject of extensive study, given the aircraft's global popularity. The wing section along the span is defined by the NACA 2412 airfoil geometry, as shown in Figure (1). This NACA 2412 profile will be utilized for the development of the present study. By defining the wing's properties, it will be possible to determine the aerodynamic loads and subsequently model the problem addressed in this work.

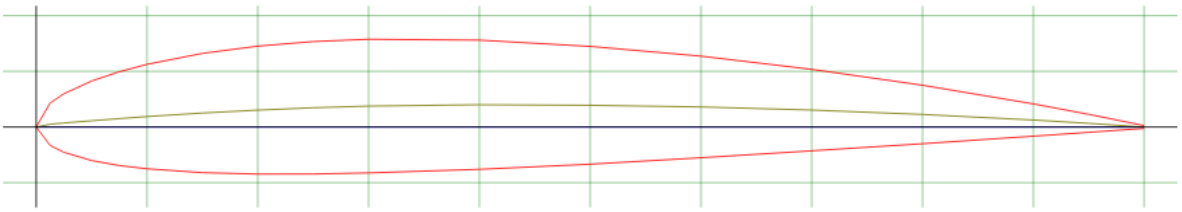


Figure 1. Perfil da corda média do Cessna 172 - NACA 2412.

Key dimensional data can be obtained from reputable sources for characterizing the wing geometry. Among the main characteristics are the chord and the wingspan. The wingspan is the distance between the wing tips measured along the wing's centerline. The chord is the distance from the leading edge to the trailing edge of the wing, measured along the wing's centerline. The chord length may vary along the wingspan, typically being larger at the wing root and smaller near the wing tip.

Schumacher [1] and Vadivelu [2] provide dimensional data for the Cessna 172 wing. Additional relevant information was obtained from the aircraft manual [3] and the performance evaluation study [4]. The main characteristics are summarized in Table 1.

Table 1. Wing characteristics.

Parameter	Value
Wingspan (b)	11 m
Mean Chord ($\bar{c}$)	1.47 m
Wing Area (S)	16.17 m²

To simplify the mathematical modeling, a wing with a constant airfoil profile along the entire span is considered. The mean chord length corresponding to the NACA 2412, representing the Cessna 172 mean chord, is used.

For the computational implementation of the NACA 2412 airfoil and subsequent calculations, the profile coordinates (X and Y) are required. These coordinates were obtained from the UIUC Airfoil Database. The data for the NACA 2412 profile are presented in Table 2, where Y_e denotes the upper surface (extrados) and Y_i the lower surface (intrados) of the wing.

Using the obtained geometric points, it is possible to estimate the wing section's moment of inertia, a key parameter for describing the structural behavior of the airfoil cross-section. According to the Department of Aeronautics and Astronautics at MIT [5], the area and moment of inertia of the wing section can be calculated solely from the coordinate points defining the airfoil, as illustrated in Figure 2.

Using the presented model, the cross-sectional area is given by Equation (1):

$$A = \int_c^0 (Y_e - Y_i)\, dx \tag{1}$$

The mean value between Y_e and Y_i is given by:

Table 2. Geometric points of the NACA 2412 airfoil

X	Y_e	Y_i
1.0000	0.0013	-0.0013
0.9500	0.0114	-0.0048
0.9000	0.0208	-0.0082
0.8000	0.0375	-0.0150
0.7000	0.0518	-0.0214
0.6000	0.0636	-0.0276
0.5000	0.0724	-0.0334
0.4000	0.0780	-0.0380
0.3000	0.0788	-0.0412
0.2500	0.0767	-0.0422
0.2000	0.0726	-0.0423
0.1500	0.0661	-0.0410
0.1000	0.0563	-0.0375
0.0750	0.0496	-0.0346
0.0500	0.0413	-0.0301
0.0250	0.0299	-0.0227
0.0125	0.0215	-0.0165
0.0000	0.0000	0.0000

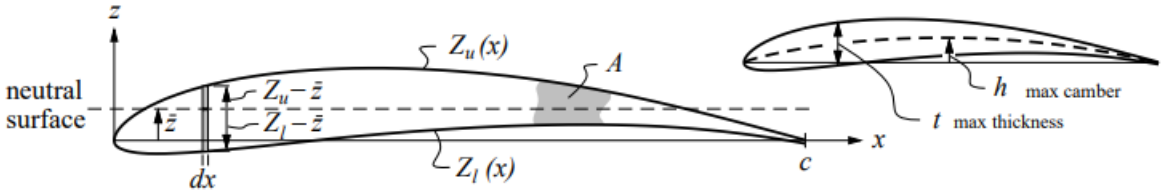


Figure 2. Estimation calculation of the moment of inertia for an airfoil section.

$$\overline{y} = \frac{1}{A}\int_c^0 \left(Y_e^2 - Y_i^2\right) dx \tag{2}$$

The moment of inertia can be calculated using Equation (3):

$$I = \int_c^0 \frac{1}{3}\left[(Y_e - \overline{y})^3 - (Y_i - \overline{y})^3\right] dx \tag{3}$$

Additionally, other parameters to be used include the thickness ratio and camber ratio, defined as:

$$\tau \equiv \frac{t}{c} \tag{4}$$

$$\epsilon_h \equiv \frac{h}{c} \tag{5}$$

To optimize the mathematical modeling, according to MIT [5], the area and moment of inertia can be approximated by Equations (6) and (7):

The area is proportional to chord and thickness:

$$A_s \approx K_A c^2 t \tag{6}$$

The moment of inertia is proportional to chord and thickness:

$$I \approx K_I c t (t^2 + h^2) \tag{7}$$

Based on data from MIT [5], for common airfoil profiles, the proportionality constants K_A and K_I approximate to:

$$K_A = 0.6 \tag{8}$$

$$K_I = 0.036 \tag{9}$$

Moreover, thickness (t) and camber (h) are defined as:

$$t = \max Y_e(x) - Y_i(x) \tag{10}$$

$$h = \max \frac{Y_e(x) + Y_i(x)}{2} \tag{11}$$

The necessary calculations were carried out to produce the data presented in Table 3:

Table 3. Thickness and camber points of the NACA 2412 profile

$Y_e(x) - Y_i(x)$	$[Y_e(x) + Y_i(x)]/2$
0.0026	0
0.0162	0.0033
0.029	0.0063
0.0525	0.01125
0.0732	0.0152
0.0912	0.018
0.1058	0.0195
0.116	0.02
0.12	0.0188
0.1189	0.01725
0.1149	0.01515
0.1071	0.01255
0.0938	0.0094
0.0842	0.0075
0.0714	0.0056
0.0526	0.0036
0.038	0.0025
0	0

From the maximum values in Table 3, using Equations (10) and (11), thickness and camber values were found, presented in Table 4:

Table 4. Thickness and camber values

Parameter	Value
t	0.1200
h	0.0200

Using Equations (1) and (3), the section area is given by Equation (6):

$$A_s \approx 0.6 \times 1.47^2 \times 0.12 = 0.1058, m^2 \tag{12}$$

The moment of inertia, from Equation (7), is:

$$I \approx 0.036 \times 1.47 \times 0.12 \times (0.12^2 + 0.02^2) = 9.3986 \times 10^{-5}, m^4 \tag{13}$$

The material chosen for the wing structure is Aluminum 6061, widely used in aerospace components due to its strength, lightness, and durability. Some of its properties, studied by Alan Hellier et al. [6], are shown in Table 5:

Table 5. Properties of Aluminum 6061

Property	Value
Young's Modulus	69 GPa
Poisson's Ratio	0.33
Ultimate Tensile Strength	310 MPa
Yield Strength	276 MPa
Density	2700 kg/m³
Elastic Modulus	200 GPa

Assuming a solid wing with uniform cross-sectional area along the span, the volume is:

$$V = A_s \times b = 0.1058 \times 11 = 0.5819, m^3 \tag{14}$$

The wing mass is:

$$m_a = \rho \times V = 2700 \times 0.5819 = 1571.13, kg \tag{15}$$

The mass of one wing half is:

$$m_{la} = \frac{m_a}{2} = 785.565, kg \tag{16}$$

However, this value is excessively high for a light aircraft wing, since the aircraft's Maximum Takeoff Weight (MTOW) is 1043.26 kg according to the manuals [4]. Treating the wing as a solid body is inaccurate because the wing is constructed with optimized lightweight structures. Therefore, although the moment of inertia is calculated assuming a solid profile, the wing mass will be taken from McIver's data [4].

Based on McIver [4] data:

$$m_{2s} = 107.05, kg \tag{17}$$

Thus, the mass of one wing half is:

$$m_s = \frac{m_{2s}}{2} = 53.52, kg \tag{18}$$

To simplify the mathematical model, the wing stiffness is approximated by modeling the wing as a cantilever beam, with stiffness given by Equation (19):

$$k = \frac{3EI}{\left(\frac{b}{2}\right)^3} \tag{19}$$

2.2 Aerodynamic Load Description Methodology

The aerodynamic load description method to be developed is based on the Hoblit model [7]. Considering that turbulence is a combination of discrete gusts, one of the premises of this study is to simplify the turbulence model into a discrete horizontal gust. Using the equations developed by Hoblit [7], the wind load acting on the structure due to the gust effect will be determined.

Assuming that during cruise flight the aircraft is in equilibrium, i.e., lift (L) equals weight (W), the resultant force from the gust action is only the variation in lift generated by the gust.

For simplification purposes, the lift load, which is distributed along the wing, will be represented as a concentrated force acting at the wing center, located at the mean aerodynamic chord profile, as shown in Figure 3.

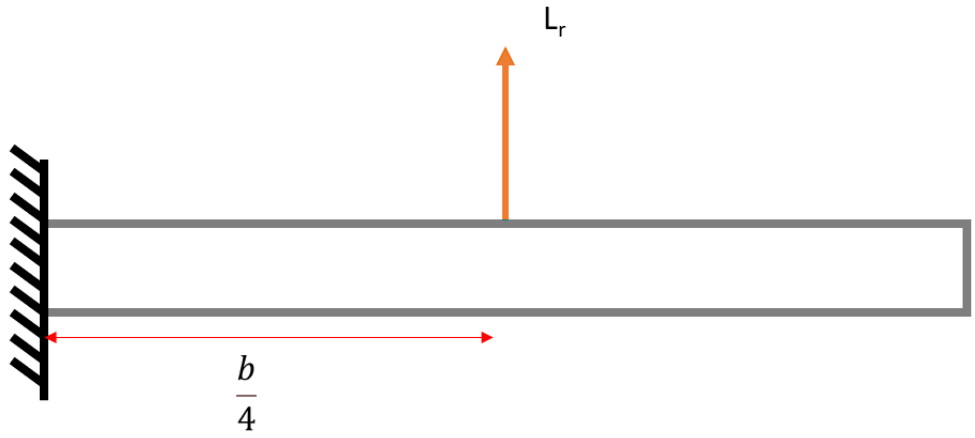


Figure 3. Frontal view of lift variation due to gust application.

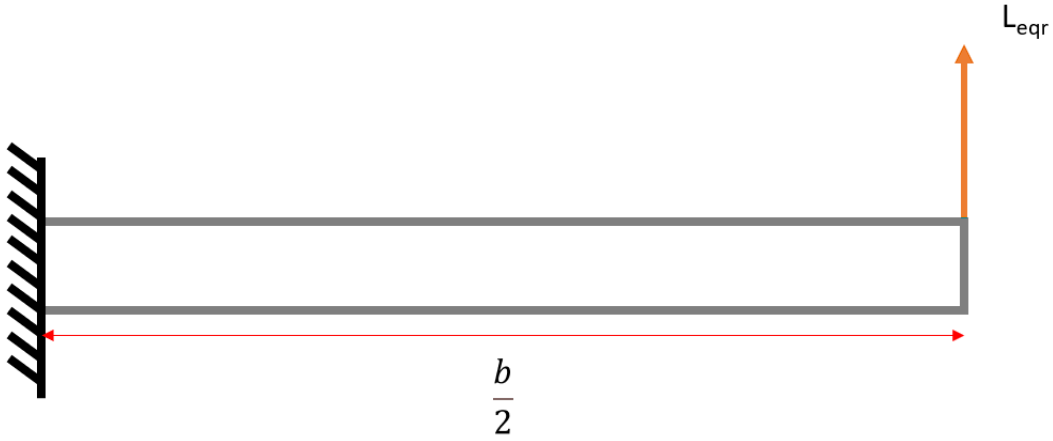


Figure 4. Frontal view of the equivalent displacement force from lift variation.

From this force, to find the displacement at the wingtip, an equivalent lift force will be calculated. This equivalent force, applied at the wingtip, will produce a displacement equal to that caused by the force applied at the wing center.

Using structural analysis concepts and modeling the wing as a beam, for the situations in Figures 3 and 4, the maximum displacements are given by:

Maximum wing displacement due to the lift variation force applied at mid-span:

$$y_c = \frac{L_r \left(\frac{b}{2}\right)^2}{6EI} \left(3\left(\frac{b}{2}\right) - \left(\frac{b}{4}\right)\right) \tag{20}$$

Maximum wing displacement due to the equivalent force applied at the wingtip:

$$y_p = \frac{L_{eqr} \left(\frac{b}{2}\right)^3}{3EI} \tag{21}$$

Equating both expressions yields the equivalent force at the wingtip as:

$$L_r = 0.3125 L_{eqr} \tag{22}$$

Based on the studied geometry, modeling will follow flight conditions described by Hoblit [7]. For the gust velocity, the aircraft's design cruise speed provided by Hoblit [7] will be used. According to FAR regulations for altitudes up to 20,000 ft, the gust wind speed is taken as $U = 50 fps$, equivalent to $U = 15.24 m/s$.

The cruise speed of a Cessna 172, according to McIver [4], is 140 mph at 8,000 ft altitude, approximately 62 m/s at 2,438.4 m.

For the lift coefficient parameter, it is assumed that at cruise flight the aircraft operates at zero angle of attack (AoA = 0°). The lift coefficient varies with the Reynolds number, a dimensionless quantity describing fluid behavior around solid objects, in this case, the wing. The Reynolds number adopted is 100,000. According to [8] and [9], the NACA2412-IL airfoil at Reynolds number 100,000 has a lift coefficient $Cl_{cr} = 0.261$.

The variation in lift force due to the gust is estimated using the standard lift equation modified for a discrete horizontal gust component. The expression is given by:

$$\Delta L = \frac{1}{2}\rho V U S Cl_{cr} \tag{23}$$

Using these data and applying Equation (23), the lift variation due to the gust is calculated as:

$$\Delta L = 3839.3992N \tag{24}$$

Using Equation (22), the equivalent load at the wingtip is:

$$\Delta L_{eqr} = 1199.8122N \tag{25}$$

This force is modeled as an impact lasting 0.1 s.

The wing stiffness matrix is given by Equation (19), yielding:

$$k_s = 116935.2487N/m \tag{26}$$

Assuming the wing is made of aluminum, based on Mevada and Patel [10] and Colakoglu [11], the typical damping ratio for aluminum is approximately 0.004 (i.e., $\xi = 0.4\%$). Thus, the damping coefficient is given by:

$$c_s = 2\xi\sqrt{k_s m_s} \tag{27}$$

Which results in:

$$c_s = 20.0134Ns/m \tag{28}$$

2.3 Numerical Integration Using the Newmark Method

The Newmark method is a numerical technique widely applied for the dynamic analysis of structures. Through this method, it is possible to simulate the response of a structure subjected to dynamic excitations, such as earthquakes, wind loads, or vibrations. The method performs a numerical integration of the equations of motion, which are formulated in terms of the internal and external forces acting on the structure. The external forces are defined by the loading functions representing the dynamic excitation, while the internal forces are determined based on the mechanical properties of the structure, such as stiffness and mass.

By developing displacement, velocity, and acceleration vectors at a given time instant, the first step of the method is to compute these quantities at the next time step, as described by equations (29)–(31):

$$u_{t+\Delta t} = u_t + \Delta u \tag{29}$$

$$\dot{u}_{t+\Delta t} = b_0\Delta u - b_2\dot{u}_t - b_3\ddot{u}_t \tag{30}$$

$$\ddot{u}_{t+\Delta t} = b_1\Delta u - b_4\dot{u}_t - b_5\ddot{u}_t \tag{31}$$

According to Brasil, Balthazar, and Góis [12], the coefficients b are defined as follows:

$$\begin{gathered} b_0 = \gamma\beta\Delta t \qquad b_1 = 1\beta\Delta t^2 \quad b_2 = \gamma\beta - 1 \\ b_3 = \Delta t2\left(\gamma\beta - 2\right) \quad b_4 = 1\beta\Delta t \quad b_5 = 12\beta - 1 \end{gathered} \tag{32}$$

These coefficients can be defined in various ways. Using the average acceleration method, it is assumed that the acceleration remains constant within the time step and equals the mean value at the step endpoints. Under this assumption, the parameters are:

$$\gamma = \frac{1}{2} \tag{33}$$

$$\beta = \frac{1}{4} \tag{34}$$

Thus, the coefficients are simplified to:

$$\begin{aligned} b_0 &= \tfrac{2}{\Delta t} \quad b_1 = \tfrac{4}{\Delta t^2} \quad b_2 = 1 \\ b_3 &= 0 \quad\;\; b_4 = \tfrac{4}{\Delta t} \quad\;\; b_5 = 1 \end{aligned} \tag{35}$$

Substituting these expressions into the equation of motion yields:

$$M\ddot{u}_{t+\Delta t} + C\dot{u}_{t+\Delta t} + Ku_{t+\Delta t} = p_{t+\Delta t} \tag{36}$$

The equivalent stiffness matrix $\hat{K}$ is given by:

$$\hat{K}\Delta u = \hat{p}_{t+\Delta t} \tag{37}$$

$$\hat{K} = b_0 M + b_1 C + K \tag{38}$$

Accordingly, considering a time increment Δt, the equivalent load vector is defined as:

$$\hat{p}_{t+\Delta t} = p_{t+\Delta t} + (b_4 M + b_3 C)\ddot{x}_t + (b_5 M + b_2 C)\dot{x}_t - Kx_t \tag{39}$$

3 Results

For the problem modeling developed in this study, the computational tool MATLAB was employed. MATLAB is a programming language and development environment for numerical computation, data visualization, and programming. This software is widely used for various engineering problems, especially in the aerospace field.

To optimize computation time and ensure functional implementation, a script containing all necessary equations for obtaining the input data was developed.

Based on the input data, a script was implemented to graphically demonstrate the wing's displacement under wind load, as presented in Figure (5).

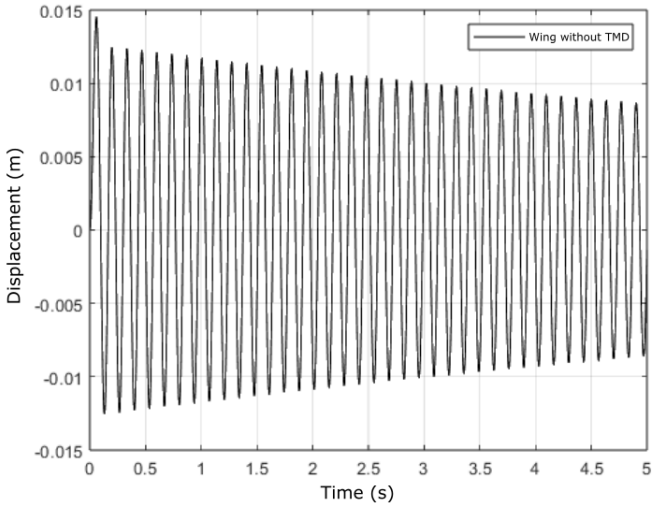


Figure 5. Wing displacement under wind load.

From Figure (5), it can be observed that during the wind impact phase (0.1 s), the wing exhibits an initial maximum displacement of 0.0145 m. After this period, the energy dissipates through damping, leading to gradually decreasing oscillation amplitudes.

To determine an optimized TMD, MATLAB's *fmincon* function was used. This function solves nonlinear constrained optimization problems. According to MathWorks [13], *fmincon* uses a Sequential Quadratic Programming (SQP) approach and may also employ Conjugate Gradient (CG) or Projected Gradient (PG) methods depending on the problem and options specified.

The developed script with *fmincon* aims to minimize wing vibration amplitudes by determining TMD parameters such as mass, stiffness, and damping.

Design constraints for the TMD parameters are given by Equations (40)–(42):

$$0.01 \cdot m_s < m_t < 0.1 \cdot m_s \tag{40}$$

$$0.01 \cdot k_s < k_t < 0.5 \cdot k_s \tag{41}$$

$$0.01 \cdot c_s < c_t < 0.5 \cdot c_s \tag{42}$$

These constraints ensure feasible design values, avoiding impractically low or excessively high parameters relative to the wing's properties. The optimized TMD values were obtained using random initial estimates and minimizing the vibration amplitudes.

Table 6. Optimized TMD parameters.

Optimized Parameter	Value
Mass (m_t)	5.321890 kg
Stiffness (k_t)	4677.461925 N/m
Damping (c_t)	9.773639 Ns/m

Iter	F-count	f(x)	Feasibility	First-order optimality	Norm of step
0	4	1.403850e-02	0.000e+00	5.995e-06	
1	8	1.403852e-02	0.000e+00	6.007e-06	1.170e-03
2	12	1.403862e-02	0.000e+00	6.084e-06	6.999e-03
3	16	1.403911e-02	0.000e+00	6.441e-06	3.240e-02
4	20	1.404093e-02	0.000e+00	7.740e-06	1.182e-01
5	24	1.404174e-02	0.000e+00	8.306e-06	5.148e-02
6	28	1.404136e-02	0.000e+00	7.368e-06	2.414e-02
7	32	1.403855e-02	0.000e+00	6.327e-06	1.831e-01
8	37	1.403469e-02	0.000e+00	4.961e-06	2.723e-01
9	42	1.403311e-02	0.000e+00	3.565e-06	1.190e-01
10	46	1.403292e-02	0.000e+00	1.946e-06	1.440e-02
11	50	1.403162e-02	0.000e+00	1.699e-06	1.023e-01
12	54	1.403151e-02	0.000e+00	1.698e-06	8.759e-03
13	58	1.403151e-02	0.000e+00	1.690e-06	2.978e-05
14	62	1.403151e-02	0.000e+00	1.698e-06	1.686e-05
15	66	1.403151e-02	0.000e+00	1.698e-06	5.496e-05
16	70	1.403151e-02	0.000e+00	1.698e-06	2.617e-04
17	74	1.403150e-02	0.000e+00	1.703e-06	1.338e-03
18	78	1.403149e-02	0.000e+00	1.697e-06	6.679e-03
19	82	1.403141e-02	0.000e+00	1.699e-06	3.323e-02
20	86	1.403105e-02	0.000e+00	1.692e-06	1.646e-01
21	90	1.402932e-02	0.000e+00	1.668e-06	7.741e-01
22	95	1.402830e-02	0.000e+00	1.503e-06	4.594e-01
23	100	1.402779e-02	0.000e+00	7.899e-07	2.309e-01

Figure 6. Optimization iterations and results.

The resulting optimized TMD parameters are summarized in Table (6). The optimization is complete because the obtained solution satisfies all constraints within the specified constraint tolerance, the objective function is non-decreasing in feasible directions, and the optimality conditions are met within the optimality tolerance, as shown by the results of the iterations in the Figure (6).

Based on the TMD data, the parameters of this device can be incorporated into the governing equation describing the displacements of a two-degree-of-freedom (2DOF) system. Using these parameters, the system dis-

placements were modeled by numerical integration employing the Newmark method. The resulting displacement time histories of the components are presented in the graphs shown in Figure (7).

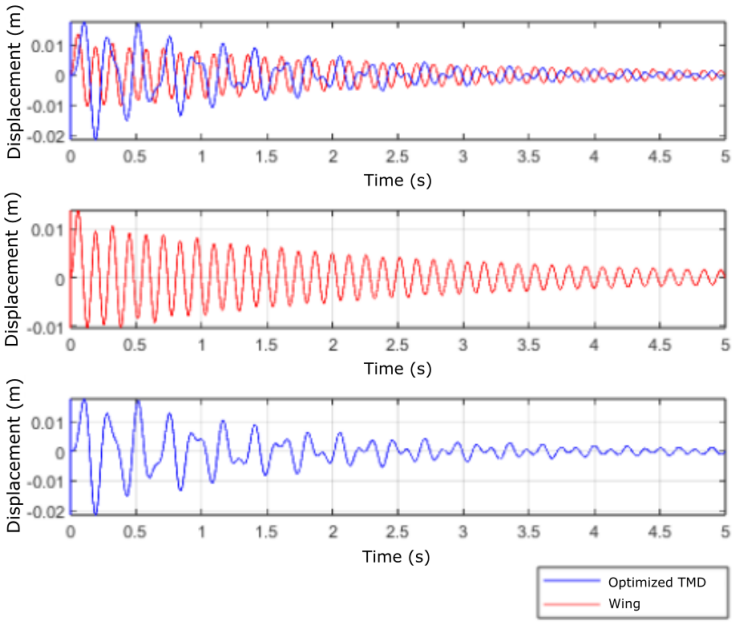


Figure 7. Displacements of wing and optimized TMD over time.

In these plots, the blue lines represent the optimized TMD; the red lines correspond to the wing equipped with the optimized TMD; and the black lines depict the wing without the TMD.

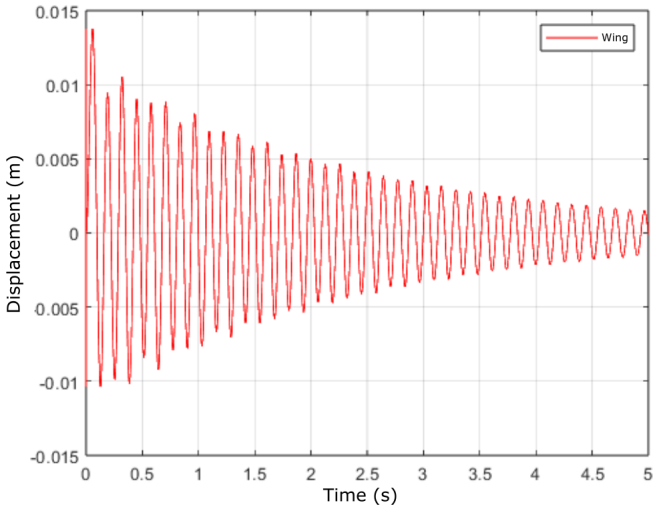


Figure 8. Wing displacement with optimized TMD.

The time history of the wing displacement, depicted in Figure (8), reveals the dynamic response of the structure to the initial aerodynamic excitation. The maximum displacement of 0.0138 m observed immediately after perturbation confirms the significant impact of the aerodynamic load. The subsequent rapid decay in vibration amplitude, reaching approximately 0.0015 m at 5 seconds, indicates effective energy dissipation within the system.

Similarly, the TMD displacement response shown in Figure (9) exhibits a peak amplitude of approximately 0.018 m, slightly higher than that of the wing, which is consistent with the expected behavior of the mass damper absorbing energy from the primary system. The TMD's vibration amplitude also decays to near 0.0015 m by the end of the 5-second interval, demonstrating its role in attenuating structural vibrations.

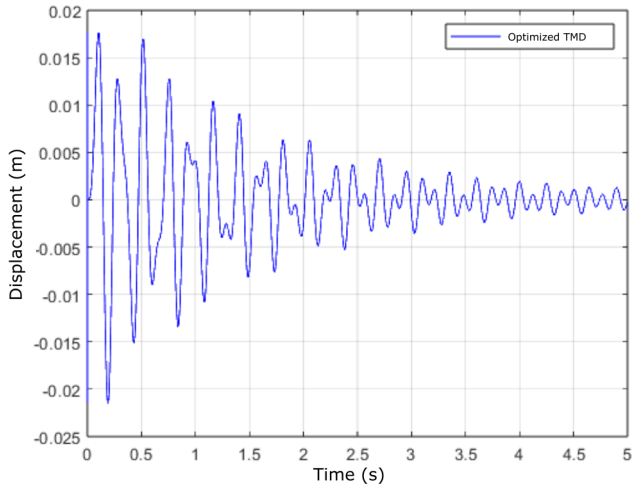


Figure 9. Optimized TMD displacement.

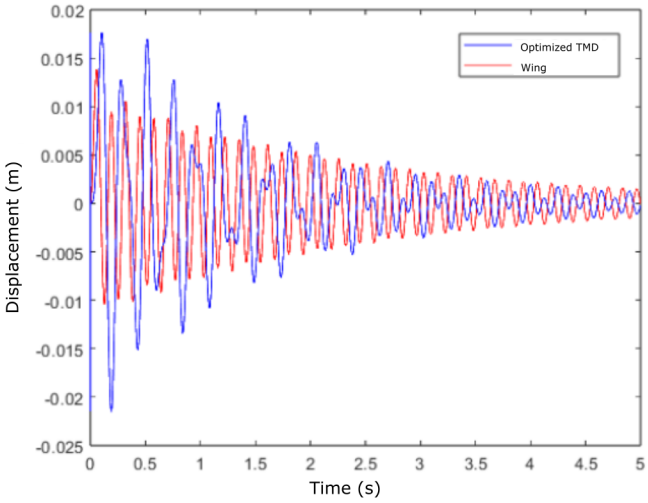


Figure 10. Wing and TMD displacement (5 s).

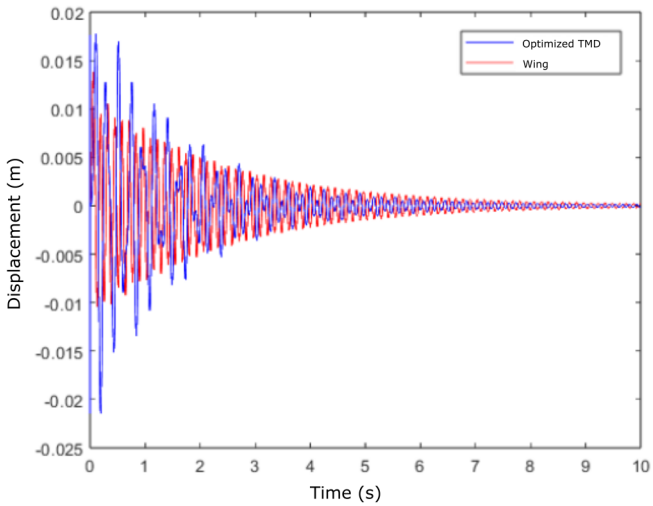


Figure 11. Wing and TMD displacement (10 s).

The coupled system behavior, illustrated by the superimposed time histories in Figure (10), confirms the synergistic damping effect between the wing and the optimized TMD. Notably, the TMD enhances the overall damping capacity, reducing vibration amplitudes more effectively than the wing alone.

Extending the simulation duration to 10 seconds, as shown in Figure (11), further substantiates the stabilization trend of the wing–TMD system. The system achieves low-amplitude vibrations within this time frame, highlighting the TMD's efficiency in accelerating the decay of oscillations.

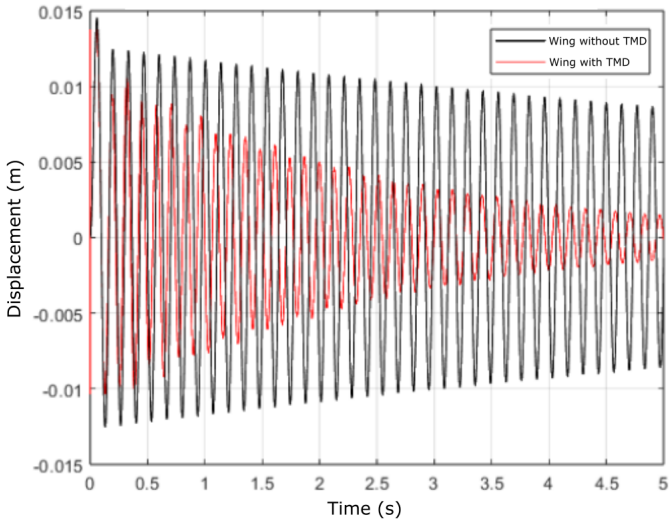


Figure 12. Wing displacement with and without TMD (5 s).

Comparative analysis between the wing with and without the TMD (Figure (12) reveals a marked improvement in damping performance when the TMD is employed. The presence of the TMD not only reduces the maximum vibration amplitude but also significantly shortens the time required for the oscillations to stabilize.

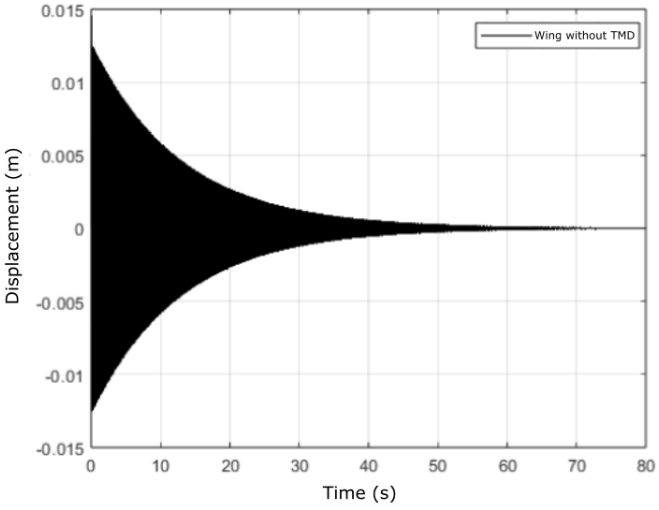


Figure 13. Wing displacement without TMD (80 s).

Longer duration simulations (Figure (14) reinforce these findings, with the wing–TMD system reaching equilibrium near 10 seconds, whereas the wing without TMD maintains substantial vibration amplitudes.

The 80-second simulation without the TMD (Figure (13) highlights the considerably prolonged stabilization period of approximately 70 seconds, underscoring the critical role of the TMD in vibration control.

Quantitatively, the optimized TMD achieved a 4.83% reduction in maximum vibration amplitude and an

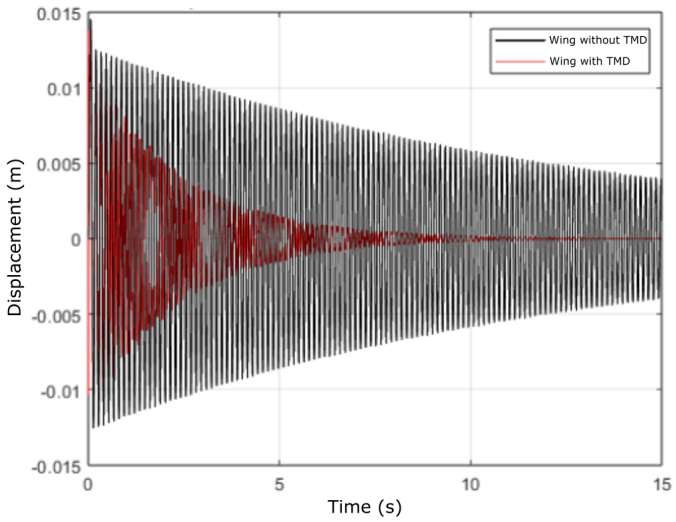


Figure 14. Wing displacement with and without TMD (15 s).

85.71% decrease in stabilization time, demonstrating its significant effectiveness in mitigating aeroelastic vibrations.

Table 7. Comparison: wing with and without optimized TMD.

	Max. Amplitude	Wing Stabilization Time
Without TMD	0.0145 m	$\approx$ 70 s
With Optimized TMD	0.0138 m	$\approx$ 10 s

4 Conclusions

The optimized Tuned Mass Damper (TMD) effectively reduces both vibration amplitude and oscillation duration in the wing structure. This reduction leads to fewer load cycles over time, potentially increasing the structural lifespan by mitigating fatigue damage. The results confirm the feasibility of applying TMDs for vibration control in aircraft wings. Future studies should focus on incorporating fluid–structure interaction, nonlinear aeroelastic effects, and realistic turbulence models to improve the accuracy and applicability of the findings.

Acknowledgements. I would like to express my sincere gratitude to Professor Dr. Marcelo Araujo da Silva for his guidance, support, and encouragement throughout the development of this work. I also acknowledge the Federal University of ABC (UFABC) for providing the academic environment and resources necessary for the completion of this project. Finally, I am deeply thankful to my family for their unconditional support and motivation during this journey.

Authorship statement. The authors hereby confirm that they are the sole liable persons responsible for the authorship of this work, and that all material that has been herein included as part of the present paper is either the property (and authorship) of the authors, or has the permission of the owners to be included here.

References

[1] A. E. Schumacher, E. Sjogren, and T. Persson. *Winglet Effect on Induced Drag for a Cessna 172 Wing*, 2014.
[2] P. Vadivelu, D. Lakshmanan, R. Naveen, K. Mathivannan, and G. Y. Kumar. *Numerical study on Longitudinal control of Cessna 172 Skyhawk aircraft by Tail arm length*. IOP Publishing, 2020.
[3] Cessna-Company. *Cessna 172 1974 Skyhawk Owner's Manual: Pilot Operating Handbook (POH) / Aircraft Flight Manual (AFM)*. Independently Published, 2018.

[4] J. McIver. *Cessna Skyhawk Performance Assessment*, 2003.
[5] MIT. Area and bending inertia of airfoil sections, 2022.
[6] A. Hellier, P. Chaphalkar, and G. Prusty. *Fracture Toughness Measurement for Aluminium 6061-T6 using Notched Round Bars*, 2017.
[7] F. M. Hoblit. *Gust Loads on Aircraft : Concepts and Applications*. AIAA education series. American Institute of Aeronautics and Astronautics, Washington D.C, 10. ed. edition, 1988.
[8] R. Kumar. *Design of NACA 2412 and its Analysis at Different Angle of Attacks, Reynolds Numbers, and a wind tunnel test*, volume 3, 2021.
[9] AirfoilTools. Naca 2412 (naca2412-il) xfoil prediction polar at re=100,000 ncrit=9, 2022.
[10] H. Mevada and D. Patel. Experimental determination of structural damping of different materials. *Procedia Engineering*, vol. 144, pp. 110–115. International Conference on Vibration Problems 2015, 2016.
[11] M. Colakoglu. *Factors effecting internal damping in aluminum*, volume 42, 2004.
[12] R. Brasil, J. Balthazar, and W. Góis. *Métodos numéricos e computacionais na prática de engenharias e ciências*. Editora Edgard Blücher Ltda, 2015.
[13] MathWorks. *Find minimum of constrained nonlinear multivariable function*, 2023.